Quantum Monte Carlo study of the S_4 symmetric microscopic model for iron-based superconductors

Guang-Kun Liu[1], Zhong-Bing Huang[2,3] and Yong-Jun Wang[1]

[1] *Department of Physics, Beijing Normal University - Beijing 100875, China*
[2] *Department of Physics, Hubei University - Wuhan 430062, China*
[3] *Beijing Computational Science Research Center - Beijing 100084, China*

arXiv:1409.2075v1 [cond-mat.str-el] 7 Sep 2014

PACS 71.10.Fd – Lattice fermion models (Hubbard model, etc.)
PACS 74.20.Rp – Pairing symmetries (other than s-wave)
PACS 75.10.-b – General theory and models of magnetic ordering

Abstract –The S_4 symmetric microscopic model with two iso-spin components has been studied via constrained-path quantum Monte Carlo simulation. Our results demonstrate a stable $(\pi, 0)$ or $(0, \pi)$ magnetic order which is significantly enhanced on increasing both the Coulomb repulsion U and Hund's coupling strength J. Also, our simulation indicates that the magnetic order tends to be in an orthomagnetic one, in which the nearest-neighbour magnetic moment are orthogonal to each other, rather than in a collinear antiferromagnetic state. Interestingly, when the system is doped away from half filling, the magnetic order is obviously elevated in the low doping density, and then significantly suppressed when more electrons are introduced. Meanwhile, we find that an A_{1g} $s_{\pm}$-wave pairing dominates all the singlet nearest-neighbour pairings, and is significantly enhanced via electron doping.

Introduction. – Iron-based superconductors (IBSCs) have triggered lots of attentions since they were discovered in 2008. Through years of intensive studies, it is widely believed that the sign-reversing s-wave, so called $s_{\pm}$-wave pairing state [1, 2], is the most probable pairing symmetry for IBSCs. However, some argues that d-wave [3, 4] or p-wave [5, 6] pairings are also possible candidates. It seems to be a reasonable strategy to find out more evidences of the exact pairing symmetry through theoretical models, and indeed several initial multi-orbital models [3, 7, 8], constructed with 2 to 5 orbitals, have been proposed to understand IBSCs. However, most researchers presuppose that models without considering all active orbitals in IBSCs are insufficient [9], which means at least 5 orbitals should be included for a "proper" model. Obviously, it is very hard for current theoretical approaches to make reliable predictions.

Interestingly, with proper considerations of the S_4 symmetry in FeX (X refers As or Se) trilayers, the building blocks of IBSCs, an effective two-orbital model has been established and proven to essentially capture the underlying low-energy physics of IBSCs [10]. Compared with other multi-orbital models for IBSCs, the S_4 model not only builds possible connections between the IBSCs and cuprates [10,11], but also offers a comprehensive and novel picture describing the complex kinematics in IBSCs: Fe $3d_{xz/yz}$-orbitals are divided into two nearly degenerate and weakly coupled groups (so called S_4 iso-spins), which are properly linked with S_4 transformation. The kinematics of each group and the hybridization between them constitute the S_4 model.

Considering the weak coupling between the two components, it is argued that the physics of only one S_4 iso-spin may capture the main features of the model. So as a first order approximation, the S_4 model can be further reduced to a single iso-spin one described by an extended one-orbital Hubbard model near half filling [10, 11]. Because of its relative simplification, most previous researches on S_4 model focus on the single iso-spin case. Using a finite-temperature quantum Monte Carlo (QMC) method, Ma *et al.* [11] have simulated the model on square lattices and demonstrated a stable $(\pi, 0)$ or $(0, \pi)$ antiferromagnetic correlation at half filling and a dominant extended-s-wave pairing over other pairings at low temperatures; while another ground-state QMC study has also confirmed this pairing symmetry in various lattices and wide range of parameters [12].

Few works concentrate on the full S_4 model with two

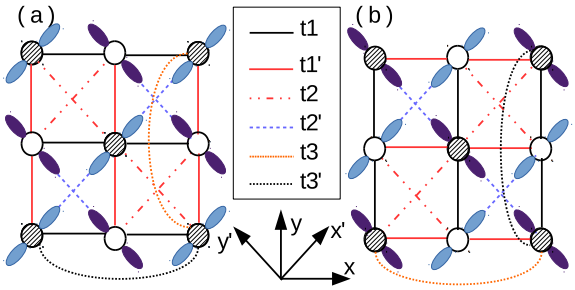

Fig. 1: A sketch of the $d_{x'z}$ and $d_{y'z}$ orbitals and schematic showing of hopping parameters for each S_4 iso-spin components. Empty and hatched circles represent different sublattice A and B, respectively. In reality, the two iso-spins overlap completely as shown in fig. 3 of ref. [10], we plot them separately for a better view of the hopping parameters in each iso-spin. It is noted that the sign of the hopping parameters are not reflected in the figure.

iso-spins, however, it would be of interest and importance to investigate how the multi-orbital interactions, such as Hund's coupling and pairing hopping, could influence the magnetic and pairing properties. In this letter, using our recently improved constrained-path quantum Monte Carlo (CPQMC) method for multi-orbital models [13], we systematically studied the magnetic order and the pairing correlation of the two-orbital S_4 symmetric microscopic model. We find a stable $(\pi, 0)$ or $(0, \pi)$ magnetic order at half filling for various Coulomb repulsion U and Hund's strength J, which are consistent with other multi-orbital models for IBSCs [13–16]. The magnetic order is obviously favoured at low electron doping and then sharply suppressed when we keep on increasing the doping density, which also agrees well with our previous QMC simulations of another two-orbital model [13]. Finally, we find that a doping-assistant $s_{\pm}$-wave pairing symmetry dominates all the pairing channels.

Model and numerical approach. – Band calculations indicate strong hybridizations between Fe 3d- and As (Se) p-orbitals near the Fermi surface, and obviously $d_{x'z}$ and $d_{y'z}$ have the largest overlaps with p'_x and p'_y orbitals along the sublattice directions x' and y' [10] (see fig. 1). Meanwhile, considering that the two As (Se) layers are separated apart along the c axis, the Fe 3d-orbitals can be divided into two single-orbital groups [10,17,18], as shown in fig. 1: One is consisted of $d_{x'z}$ on sublattice A and $d_{y'z}$ on sublattice B, and these two obitals strongly couple to the p-orbitals of the upper As (Se) layer. Comparatively, the other group has $d_{y'z}$ on sublattice A and $d_{x'z}$ on sublattice B, but couple to the lower As (Se) layer. These two iso-spins are degenerate and weakly coupled, and can be mapped into each other via S_4 transformation.

Based on these assumptions, the S_4 symmetric microscopic model can be constructed as a combination of the kinematics of the two iso-spins and the hybridization between them. Specifically, the kinetic Hamiltonian of the S_4 model can be expressed as [10]

$$
\begin{aligned}
H_{\rm kin} &= H^1_{\rm kin} + H^2_{\rm kin} + H^c_{\rm kin}, && (1)\\
H^1_{\rm kin} &= t_1 \sum_{\mathrm{i}\sigma} (a^\dagger_{\mathrm{i},1,\sigma} b_{\mathrm{i}+\hat{x},1,\sigma} + \mathrm{h.c.}) && (2)\\
&\quad + t'_1 \sum_{\mathrm{i}\sigma} (a^\dagger_{\mathrm{i},1,\sigma} b_{\mathrm{i}+\hat{y},1,\sigma} + \mathrm{h.c.})\\
&\quad + t_2 \sum_{\mathrm{i}\sigma} (a^\dagger_{\mathrm{i},1,\sigma} a_{\mathrm{i}\pm(\hat{x}+\hat{y}),1,\sigma} + b^\dagger_{\mathrm{i},1,\sigma} b_{\mathrm{i}\pm(\hat{x}-\hat{y}),1,\sigma})\\
&\quad + t'_2 \sum_{\mathrm{i}\sigma} (a^\dagger_{\mathrm{i},1,\sigma} a_{\mathrm{i}\pm(\hat{x}-\hat{y}),1,\sigma} + b^\dagger_{\mathrm{i},1,\sigma} b_{\mathrm{i}\pm(\hat{x}+\hat{y}),1,\sigma})\\
&\quad + t_3 \sum_{\mathrm{i}\sigma} (a^\dagger_{\mathrm{i},1,\sigma} a_{\mathrm{i}\pm 2\hat{x},1,\sigma} + b^\dagger_{\mathrm{i},1,\sigma} b_{\mathrm{i}\pm 2\hat{x},1,\sigma})\\
&\quad + t'_3 \sum_{\mathrm{i}\sigma} (a^\dagger_{\mathrm{i},1,\sigma} a_{\mathrm{i}\pm 2\hat{y},1,\sigma} + b^\dagger_{\mathrm{i},1,\sigma} b_{\mathrm{i}\pm 2\hat{y},1,\sigma})\\
H^2_{\rm kin} &= -t'_1 \sum_{\mathrm{i}\sigma} (a^\dagger_{\mathrm{i},2,\sigma} b_{\mathrm{i}+\hat{x},2,\sigma} + \mathrm{h.c.}) && (3)\\
&\quad - t_1 \sum_{\mathrm{i}\sigma} (a^\dagger_{\mathrm{i},2,\sigma} b_{\mathrm{i}+\hat{y},2,\sigma} + \mathrm{h.c.})\\
&\quad - t'_2 \sum_{\mathrm{i}\sigma} (a^\dagger_{\mathrm{i},2,\sigma} a_{\mathrm{i}\pm(\hat{x}+\hat{y}),2,\sigma} + b^\dagger_{\mathrm{i},2,\sigma} b_{\mathrm{i}\pm(\hat{x}-\hat{y}),2,\sigma})\\
&\quad - t_2 \sum_{\mathrm{i}\sigma} (a^\dagger_{\mathrm{i},2,\sigma} a_{\mathrm{i}\pm(\hat{x}-\hat{y}),2,\sigma} + b^\dagger_{\mathrm{i},2,\sigma} b_{\mathrm{i}\pm(\hat{x}+\hat{y}),2,\sigma})\\
&\quad + t'_3 \sum_{\mathrm{i}\sigma} (a^\dagger_{\mathrm{i},2,\sigma} a_{\mathrm{i}\pm 2\hat{x},2,\sigma} + b^\dagger_{\mathrm{i},2,\sigma} b_{\mathrm{i}\pm 2\hat{x},2,\sigma})\\
&\quad + t_3 \sum_{\mathrm{i}\sigma} (a^\dagger_{\mathrm{i},2,\sigma} a_{\mathrm{i}\pm 2\hat{y},2,\sigma} + b^\dagger_{\mathrm{i},2,\sigma} b_{\mathrm{i}\pm 2\hat{y},2,\sigma})\\
H^c_{\rm kin} &= t_c \sum_{\mathrm{i}\eta\sigma} (a^\dagger_{\mathrm{i},1,\sigma} b_{\mathrm{i}+\eta,2,\sigma} + \mathrm{h.c.}), && (4)
\end{aligned}
$$

where $a^\dagger_{\mathrm{i},\alpha,\sigma}$ ($a_{\mathrm{i},\alpha,\sigma}$) creates (annihilates) an electron with spin-σ at site $\mathrm{R_i}$ on the sublattice A for the iso-spin α ($\alpha = 1, 2$), and similarly $b^\dagger_{\mathrm{i},\alpha,\sigma}$ ($b_{\mathrm{i},\alpha,\sigma}$) acts on sublattice B. The index $\eta = \hat{x}$ or $\hat{y}$ denotes a unit vector linking the nearest-neighbour sites. Following ref. [10], the typical hopping parameters for iron pnictides will always be chosen as $t_1 = 0.37$, $t'_1 = 0.43$, $t_2 = 0.90$, $t'_2 = -0.3$, $t_3 = 0.0$, $t'_3 = 0.1$ and $t_c = 0.02$ in our simulations.

The interaction Hamiltonian $H_{\rm int}$, containing a Hubbard repulsion U within the same iso-spin, a repulsion U' for different iso-spins, a ferromagnetic Hund's coupling J and pair-hopping terms, can be written as

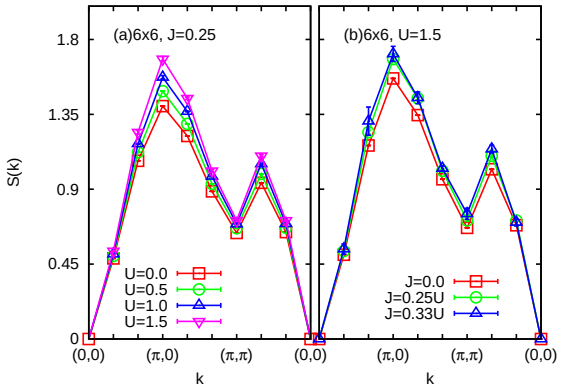

Fig. 2: Magnetic structure factor $S(k)$ at half filling on a 6×6 lattice versus various (a) U and (b) Hund's coupling J.

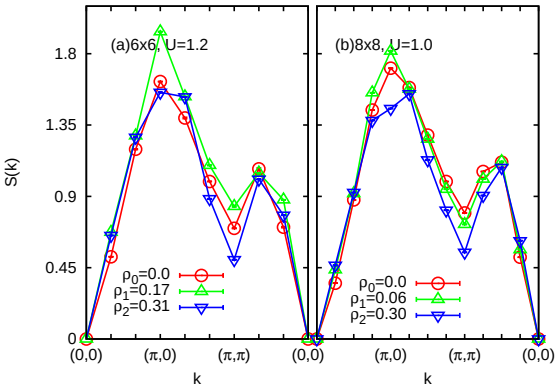

Fig. 3: (a) Magnetic structure factor $S(k)$ of (a) 6×6 and (b) 8×8 lattices on three typical electron doping densities.

$$
\begin{aligned}
H_{\rm int} =& J\sum_{\mathrm{i},\alpha\neq\alpha'}(d^\dagger_{\mathrm{i}\alpha\uparrow}d^\dagger_{\mathrm{i}\alpha'\downarrow}d_{\mathrm{i}\alpha\downarrow}d_{\mathrm{i}\alpha'\uparrow}\\
&+d^\dagger_{\mathrm{i}\alpha\uparrow}d^\dagger_{\mathrm{i}\alpha\downarrow}d_{\mathrm{i}\alpha'\downarrow}d_{\mathrm{i}\alpha'\uparrow})\\
&+(U'-J)\sum_{\mathrm{i},\sigma}n_{\mathrm{i},1,\sigma}n_{\mathrm{i},2,\sigma}\\
&+U\sum_{\mathrm{i},\alpha}n_{\mathrm{i}\alpha\uparrow}n_{\mathrm{i}\alpha\downarrow}+U'\sum_{\mathrm{i},\sigma}n_{\mathrm{i},1,\sigma}n_{\mathrm{i},2,-\sigma},
\end{aligned}
\tag{5}
$$

where $d^\dagger_{i,\alpha,\sigma}$ ($d_{i,\alpha,\sigma}$) creates (annihilates) a spin-σ electron at site $\mathrm{R_i}$ (sublattice A or B) for iso-spin α ($\alpha=1,2$), and U' satisfies the constraint $U'=U-2J$ due to the rotational invariance [19].

We employ the CPQMC method [20] to study the system. In the CPQMC method, like other projector ground state QMC method, the ground state, represented by a Slater determinant $|\phi_g\rangle$, can be projected iteratively from any non-orthogonal, initial state $|\phi_t\rangle$ via branching random walks in the overcomplete Slater determinant space — $|\phi^{n+1}\rangle = e^{-\Delta\tau H}|\phi^n\rangle$ with $|\phi^0\rangle \equiv |\phi_t\rangle$ and H being the Hamiltonian. Differently, CPQMC requires every random walker $|\phi^n\rangle$ in the iterations obey the restriction $\langle\phi_t|\phi^n\rangle > 0$. If the initial state happened to be the ground state of the system, $|\phi_t\rangle = |\phi_g\rangle$, no sign problem would ever appear under $\langle\phi_t|\phi^n\rangle > 0$ [20]. Obviously, such an ideal situation never occurs in practical simulations. But even under the approximate restriction $\langle\phi_t|\phi^n\rangle > 0$, CPQMC still efficiently eliminates the infamous Fermi sign problem and obtains very high accurate results [20,21].

In the usual CPQMC algorithm, before the projecting iteration $|\phi^{n+1}\rangle = e^{-\Delta\tau H}|\phi^n\rangle$, we often transform $e^{-\Delta\tau H}$ into combinations of simple items that can be easily handled with, for example, we decouple the $e^{-\Delta\tau U n_{i\uparrow}n_{i\downarrow}}$ into $e^{-\Delta\tau U(n_{i\uparrow}+n_{i\downarrow})/2}\sum_{\sigma=\pm1}e^{\gamma\sigma(n_{i\uparrow}-n_{i\downarrow})}$ via discrete Hubbard-Stranovich (HS) transformation [22]. However, considering the much more complex interaction items in the two-orbital system, such as $H_1 = J\sum_{\alpha\neq\alpha'}(d^\dagger_{\mathrm{i}\alpha\uparrow}d^\dagger_{\mathrm{i}\alpha'\downarrow}d_{\mathrm{i}\alpha\downarrow}d_{\mathrm{i}\alpha'\uparrow} + d^\dagger_{\mathrm{i}\alpha\uparrow}d^\dagger_{\mathrm{i}\alpha\downarrow}d_{\mathrm{i}\alpha'\downarrow}d_{\mathrm{i}\alpha'\uparrow})$, it is rather difficult to implement the HS transformation in QMC simulation, since it would induce a rather severe sign problem even for CPQMC method.

In order to solve this problem, we adopt a new transformation for $e^{-\Delta\tau H_1}$, which can sufficiently suppress the sign problem in a wide regime of parameters [23], and develop the two-orbital CPQMC algorithm for the S_4 model. In our simulations, $e^{-\Delta\tau H_1}$ is decoupled as,

$$
e^{-\Delta\tau H_1} = \frac{1}{2}\sum_{\gamma=\pm1}e^{\lambda\gamma(f_{\mathrm{i}\uparrow}-f_{\mathrm{i}\downarrow})}e^{a(N_{\mathrm{i}\uparrow}+N_{\mathrm{i}\downarrow})+bN_{\mathrm{i}\uparrow}N_{\mathrm{i}\downarrow}} \tag{6}
$$

with

$$
f_{\mathrm{i},\sigma} = d^\dagger_{\mathrm{i},x,\sigma}d_{\mathrm{i},y,\sigma}+d^\dagger_{\mathrm{i},y,\sigma}d_{\mathrm{i},x,\sigma}, \tag{7}
$$

$$
N_{\mathrm{i},\sigma} = n_{\mathrm{i},x,\sigma}+n_{\mathrm{i},y,\sigma}-2n_{\mathrm{i},x,\sigma}n_{\mathrm{i},y,\sigma}, \tag{8}
$$

where a, b and λ are functions of J and $\Delta\tau$, and $\gamma = \pm1$ is the newly introduced auxiliary field [23]. For more CPQMC calculation details for the two-orbital model, see ref. [13].

Results. – We first investigate the magnetic properties of the model at half filling. In fig. 2, the magnetic structure factor, $S(\mathrm{k}) = \frac{1}{N}\sum_{ij}e^{i\mathrm{k}\cdot(\mathrm{r}_i-\mathrm{r}_j)}\langle(n_{\mathrm{i}\uparrow}-n_{\mathrm{i}\downarrow})(n_{\mathrm{j}\uparrow}-n_{\mathrm{j}\downarrow})\rangle$ with $n_{i\sigma}$ being the number operator, is illustrated for various Coulomb repulsion U and the Hund's coupling J. From fig.2(a), we can see that $S(\pi,0)$ takes a maximum over all the high-symmetry k-points along the $(0,0)$–$(\pi,0)$–(π,π)–$(0,0)$, and such a maximum is significantly enhanced on increasing U with a fixed $J=0.25U$. Similarly, with a given U, as shown in fig.2(b), the Hund's coupling J also slightly strengthens this $(\pi,0)$ or $(0,\pi)$ magnetic order. The property is consistent with previous Lanczos and QMC studies [13,16,24] for another two-orbital model [7].

Next we calculate the magnetic structure factor at various electron dopings. In fig. 3, three typical doping cases

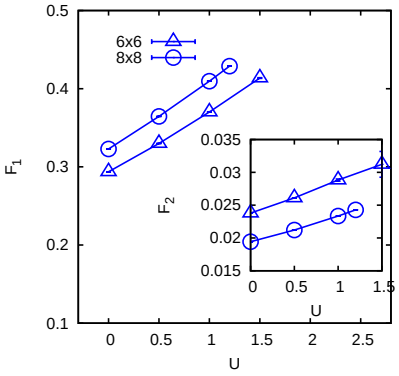

Fig. 4: Four-spin-operators $F_1 = \langle \vec{S}_i^2 \rangle^2 - \langle (\vec{S}_i \cdot \vec{S}_{i+\hat{x}})^2 \rangle$ and $F_2 = \langle (\vec{S}_i \cdot \vec{S}_{i+\hat{x}+\hat{y}})^2 \rangle - \langle (\vec{S}_i \cdot \vec{S}_{i+\hat{x}})^2 \rangle$ versus Coulomb repulsion U on 6×6 and 8×8 lattices in half filling with $J = 0.25U$.

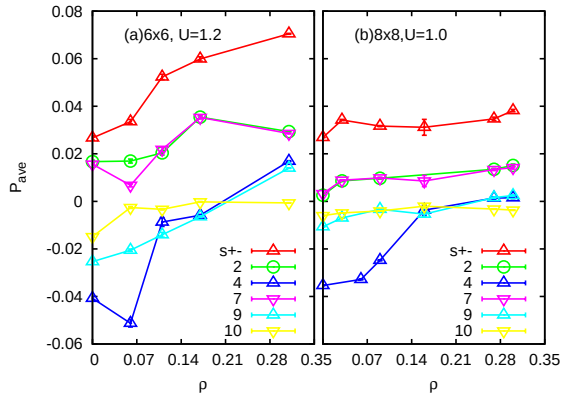

Fig. 5: Average of long-range pairing correlation $P_{\rm ave}$ versus various doping ρ on (a) a 6×6 lattice with $U = 1.2$ and $J = 0.25U$ and (b) an 8×8 lattice with $U = 1.0$ and $J = 0.25U$. We follow the classification of pairings in ref. [25] with the same meaning for the numbering.

are plotted for 6×6 and 8×8 lattices: the undoped ρ_0, the doping density ρ_1 at which the system reaches the strongest magnetic order, and the doping density ρ_2 near 30%. Interestingly, when the system is doped away from half filling, in both the 6×6 and 8×8 lattices we find that the $(\pi, 0)$ or $(0, \pi)$ magnetic order is manifestly favoured in the low doping regime (ρ_0, ρ_1), and then significantly suppressed when more electrons are doped into the system. These results also qualitatively agree with the previous QMC study [13] of the two-orbital model [7].

Considering the rich magnetic orders at half filling for IBSCs, we examine the competition between orthomagnetic (OM) [26] and collinear antiferromagnetic (AFM) [27] orders at half filling in the S_4 model. However, the OM order, which has the nearest-neighbour magnetic moments mutually-perpendicular with each other, behaves so similarly with the collinear AFM order in the numerical way [24]: They have similar magnetic structures, almost the same expected values of the nearest-neighbour and next-nearest-neighbour spin-spin correlations. In order to distinguish these two magnetic orders, two four-spin-quantities, $F_1 = \langle \vec{S}_i^2 \rangle^2 - \langle (\vec{S}_i \cdot \vec{S}_{i+\hat{x}})^2 \rangle$ and $F_2 = \langle (\vec{S}_i \cdot \vec{S}_{i+\hat{x}+\hat{y}})^2 \rangle - \langle (\vec{S}_i \cdot \vec{S}_{i+\hat{x}})^2 \rangle$, are introduced and computed. It is argued that if the system prefers the OM phase when increasing the Coulomb repulsion U, both F_1 and F_2 would go up monotonously with U [13].

In fig. 4, F_1 and F_2 are shown for various Coulomb repulsion U on different lattices. It is obvious that on both the 6×6 and 8×8 lattices, F_1 and F_2 are elevated significantly when U increases, which indicts that the system tends to be in the OM phase rather than the collinear AFM order when the electron correlation becomes stronger. Similar results are observed in previous QMC [13] and density matrix renormalization group [28] studies.

Lastly, we discuss the pairing properties of the system. Given that the pairing correlations within the first few distances dominate over the long-range ones and only reflect local correlations among spin and charge [29, 30], partial average of the pairing correlations with distances longer than 2 lattice spacing, $P_{\rm ave} = \frac{1}{M} \sum_{r>2} P(r)$ with M being the number of pairs and $P(r = |\mathrm{i} - \mathrm{j}|) = \langle \Delta^\dagger(\mathrm{i}) \Delta(\mathrm{j}) \rangle$, would be an appropriate quantity to capture the long-range pairing properties of the system. We mainly use $P_{\rm ave}$ to describe the pairing tendency of the system, and for the detailed definition of $\Delta^\dagger(\mathrm{i})$ for the two-orbital model, see the discussions in refs. [13, 14, 24, 25].

All the possible nearest-neighbour singlet pairings [13, 25] and an $s_\pm$ channel with next-nearest-neighbour pairing [13, 24] are calculated on 6×6 and 8×8 lattices at various dopings and Coulomb repulsions. In fig. 5, we can see that the $s_\pm$-wave pairing dominates all the pairings for both the 6×6 and 8×8 lattices under various dopings.

In addition, we find that almost all the pairings are enhanced as more electrons are doped into the system, especially for the $s_\pm$ channel. This result is different from our previous Monte Carlo study of another two-orbital model in which the electron doping slightly suppresses all the pairing channels [13].

Combined with the pictures of the magnetic (fig. 3) and pairing (fig. 5) properties, we can hardly find an obvious connection between the magnetic order and pairing behaviours, since the pairing correlations are simply enhanced in the whole doping regime, no matter whether the magnetic order is strengthened or weakened after doping.

Conclusion. – In summary, we have systemically studied the two-orbital S_4 symmetric microscopic model using the CPQMC method. Our simulations demonstrate a stable $(\pi, 0)$ or $(0, \pi)$ magnetic order at half filling. Such a magnetic order is stably enhanced on increasing the Coulomb repulsion U and Hund's coupling strength J, which is consistent with previous works on other two-orbital models.

Interestingly, when the system is doped away from half filling, the magnetic order is obviously enhanced at low doping densities and then sharply suppressed as more elec-

trons are introduced. We also find that the system tends to be in the OM order upon increasing Coulomb repulsion U. As for the pairing properties, our simulations strongly suggest that the $s_{\pm}$-wave pairing is the most probable candidate.

* * *

We thank Beijing Computational Research Center for sharing the computing resources. ZBH was supported by NSFC under Grants Nos. 11174072 and 91221103, and by SRFDP under Grant No. 20104208110001.

REFERENCES

[1] Mazin I.I.,Singh D.J., Johannes M.D., and Du M.H., *Phys. Rev. Lett.*, **101** (2008) 057003
[2] Chubukov A.V., Vavilov M.G., and Vorontsov A.B., *Phys. Rev. B*, **80** (2009) 140515
[3] Kuroki K., Onari S., Arita R., Usui H., Tanaka Y., Kontani H. and Aoki H., *Phys. Rev. Lett.*, **101** (2008) 087004
[4] Graser S., Maier T.A., Hirschfeld P.J., and Scalapino D.J., *New J. Phys.*, **11** (2009) 025016
[5] Lee P. and Wen X.-G., *Phys. Rev. B*, **78** (2008) 144517
[6] Brydon P.M.R., Daghofer M., Timm C., and J. Van den Beek, *Phys. Rev. B*, **83** (2011) 060501
[7] Raghu S., Qi X.-L., Liu C.-X., Scalapino D.J., and Zhang S.-C., *Phys. Rev. B*, **77** (2008) 220503
[8] Daghofer M., Nicholson A., Moreo A. and Dagotto E., *Phys. Rev. B*, **81** (2010) 014511
[9] Johnston D., *Adv. Phys.*, **59** (2010) 803
[10] Hu J. and Hao N., *Phys. Rev. X*, **2** (2012) 021009
[11] Ma T., Lin H.Q. and Hu J., *Phys. Rev. Lett.*, **110** (2013) 107002
[12] Wu Y., Liu G. and Ma T., *EPL*, **104** (2013) 27013
[13] Liu G.-K., Huang Z.-B., and Wang Y.-J., *J. Phys.: Condens. Matter*, **26** (2014) 325601
[14] Moreo A., Daghofer M., Nicholson A., and Dagotto E., *Phys. Rev. B*, **80** (2009) 104507
[15] Nicholson A., Ge W., Riera J., Daghofer M., Moreo A., and Dagotto E., *Phys. Rev. B*, **85** (2012) 024532
[16] Daghofer M., Moreo A., Riera J.A., Arrigoni E., Scalapino D.J., and Dagotto E., *Phys. Rev. Lett.*, **101** (2008) 237004
[17] Hao N., Wang Y. and Hu J., *EPL*, **104** (2013) 57007
[18] Hu J., *Journal of Physics: Conference Series*, **449** (2013) 012017
[19] Dagotto E., Hotta T. and Moreo A., *Physics Reports*, **344** (2001) 1
[20] Zhang S., Carlson J., and Gubernatis J.E., *Phys. Rev. B*, **55** (1997) 7464
[21] Zhang S., Carlson J., and Gubernatis J.E., *Phys. Rev. Lett.*, **78** (1997) 4486
[22] Hirsch J.E., *Phys. Rev. B*, **28** (1983) 4059
[23] Sakai S., Arita R. and Aoki H., *Phys. Rev. B*, **70** (2004) 172504
[24] Moreo A., Daghofer M., Riera J.A., and Dagotto E., *Phys. Rev. B*, **79** (2009) 134502.
[25] Wan Y., and Wang Q.-H., *EPL*, **85** (2009) 57007.
[26] Lorenzana J., Seibold G., Ortix C., and Grilli M., *Phys. Rev. Lett.*, **101** (2008) 186402.
[27] Dai P., Hu J. and Dagotto E., *Nat. Phys.*, **8** (2012) 709.
[28] Berg E., Kivelson S.A., and Scalapino D.J., *Phys. Rev. B*, **81** (2010) 172504
[29] Huang Z.B., Lin H.Q., and Gubernatis J.E., *Phys. Rev. B*, **63** (2001) 115112
[30] Huang Z.B., Lin H.Q., and Gubernatis J.E., *Phys. Rev. B*, **64** (2001) 205101.